

## AN EXPERIMENTAL STUDY ON THE BEHAVIOUR OF GLASS FILLED POLYPROPYLENE AND POLYETHYLENE COMPOSITE PIPES UNDER QUASI-STATIC AXIAL LOADING

### Article history

Received  
16 January 2015  
Received in revised form  
24 March 2015  
Accepted  
15 March 2015

H. H. Ya\*, and H. EL-Sobky

Universiti Teknologi PETRONAS, Bandar Seri Iskandar,  
32610 Seri Iskandar, Perak Darul Ridzuan, Malaysia

\*Corresponding author  
hamdan.ya@petronas.com.my

### Abstract

The behaviour of extruded glass fibre reinforced thermoplastic pipes under axial crushing load was investigated experimentally. It was envisaged that the difference between the axial and hoop moduli and strengths as well as the volume fraction would influence the mode of collapses and energy absorption. The moduli could be varied using a new extrusion technology, which controls the fibre orientation pattern, hence, the mechanical properties. The ability to vary the moduli and the fibre volume fraction provides means of controlling the collapse mode in order to optimize specific energy absorption. Axial compression tests were performed on glass filled Polypropylene (GPP) and glass filled Polyethylene (GPE) composite pipes. The samples were chosen with a variety of fibre volume fraction ( $V_f = 5\%$  to  $20\%$  and average angle of orientation  $\theta = 50^\circ$  to  $80^\circ$ ) to evaluate the effect of anisotropy and  $V_f$  to the collapse modes when subjected to axial static loading. The results from the experiments revealed that typical axial and hoop modulus ( $E_a$  and  $E_\theta$ ) of GPP and GPE pipes increased with increasing of  $\theta$  from  $55^\circ$  to  $75^\circ$  and decreased gradually in between  $75^\circ$  to  $80^\circ$ . The axial modulus was increased constantly with the increase of  $V_f$  from  $5\%$  to  $20\%$ . However, the hoop modulus is the highest at  $5\% V_f$ , decreases significantly at  $10\%$ , and gradually increases at  $20\%$ . It is noticed that, the GPP and GPE pipes contain higher  $V_f$  and  $\theta$ , collapsed in brittle failure mode (fragmentation), whereas those with less  $V_f$  and  $\theta$  angle, collapsed in non-axis-symmetric (diamond) mode with the local fracture while the local fracture disappeared with lower fibre contents.

Keywords: Glass filled polypropylene and polyethylene composite pipe, energy absorption, volume of fraction, fiber orientation, collapse mode

### Abstrak

Kelakuan gentian kaca bertetulang tersemerit paip termoplastik di bawah beban menghancurkan paksi disiasat melalui uji kaji. Modulus diubah dengan menggunakan teknologi penyemperitan baru, yang mengawal corak orientasi gentian, dengan itu, sifat-sifat mekanik. Ujian mampatan paksi telah dilakukan ke atas GPP dan kaca GPE paip komposit. Sampel telah dipilih dengan pelbagai pecahan isipadu gentian ( $V_f = 5\%$  kepada  $20\%$  dan sudut purata orientasi  $\theta = 50^\circ$  hingga  $80^\circ$ ). Hasil eksperimen menunjukkan bahawa paksi biasa dan gelung modulus ( $E_a$  dan  $E_\theta$ ) GPP dan GPE paip meningkat dengan peningkatan  $\theta$  daripada  $55^\circ$  hingga  $75^\circ$  dan menurun secara beransur-ansur di antara  $75^\circ$  hingga  $80^\circ$ . Modulus paksi telah meningkat sentiasa dengan peningkatan  $V_f$   $5\%$  kepada  $20\%$ . Walau bagaimanapun, modulus gelung adalah tertinggi di  $5\% V_f$ , berkurangan dengan ketara di the  $10\%$ , dan secara beransur-ansur meningkat pada  $20\%$ . Ia menyedari bahawa, GPP dan GPE paip mengandungi lebih tinggi  $V_f$  dan  $\theta$ , runtuh dalam mod kegagalan rapuh (pemecahan), dan bukannya mereka yang kurang  $V_f$  dan  $\theta$  angle runtuh dalam bukan-paksi simetri mod (berlian) dengan patah tempatan.

Kata kunci: Kaca diisi polipropilena dan polietilena paip komposit, penyerapan tenaga, jumlah pecahan, orientasi gentian, mod runtuh

© 2015 Penerbit UTM Press. All rights reserved

## 1.0 INTRODUCTION

Since the mid-20th century there have been much published research data on the response of composite tubes under axial crushing load [1-3]. Most of the work was concerned with the use of composites in applications where energy absorption under crush conditions was an important requirement [4-9]. In general, most of the composite materials, especially thermosetting fibre-reinforced polymers (FRPs), do not exhibit ductile failures associated with metals and most thermoplastics. Several authors [3-6] found that the composite materials exhibit high-energy absorption capability if the proper failure mechanism is initiated and maintained during the crush event. Interestingly, metals absorb energy primarily through plastic deformation, whereas composite materials absorb energy through a variety of failure mechanisms.

Generally, the total energy absorption capability of composite structures depends on the principal geometrical and physical parameters. A number of authors [10-17] reported that the principal geometrical parameters such as the matrix material, fibre material and fibre orientation affect the energy capability of the composite tubes. Several authors [18, 19] reported the actual fracture mode of composite tubes to be strongly dependent on the fibre arrangements. However, the optimum arrangement of fibres for structural strength and stiffness is the same as for maximum energy absorption.

Farley [4] studied the effects of fibres and matrix strain on the energy absorption of graphite-reinforced composite materials. He reported that the relative values of the fibres and matrix failure strain significantly affected the amount of energy absorption. He also suggested using the matrix materials with a higher failure strain than that of fibre reinforcement, in order to achieve the maximum energy absorption from an FRP. Farley [13] stated that the orientation criteria of the fibres in FRP composite tubes really affect the mechanical properties and enhance the energy absorption performance.

Farley [19] reported that the energy absorption capabilities of carbon-epoxy and aramid-epoxy composite tubes were non-linear function of the inside diameter to wall thickness ratio ( $D/t$ ). He noted that the energy absorption capability of composite tubes increases as the  $D/t$  decreases. A similar finding was also revealed by Mamalis [17] and Farley [20] during their investigation on the glass-polyester and near-ellipse cross-section of composite tubes.

Late in the last decade, many researchers studied aggressively the energy absorption capability of various FRP composite tubes under axial compression. The reports mentioned that the FRP composite tubes show substantial energy absorption; even when compared to aluminium and steel tubes. However, most of the previous researchers concentrated on studying the unidirectional lamina of fibres for various composite tubes.

The objective of the study as reported here is to study and investigate the specific energy absorption, post-crushing integrity and mode of failure of composite plastic pipes subjected to axial static crushing. An experimental program adopted from previous work [1, 13, 15, 17, 19] was carried out to investigate the crushing capabilities and failure modes of Medium Density Polyethylene (MDPE), Glass Polypropylene (GPP) and Glass Polyethylene (GPE) composite pipes. The GPP and GPE composite pipes were made from chopped glass fibre and polymer resin (i.e. Polypropylene /PP and Polyethylene/PE, respectively) by extrusion process in appropriate diameters according to manufacturer's specification.

## 2.0 MATERIALS AND METHODOLOGY

The LDPE, GPP and GPE composite pipes configuration was selected for the specimen in this study on the basis of stability—special produced by factory and for comparisons with other available FRP pipes obtained commercially. Chopped glass fibres (industrial E-glass) as the fibres, and MDPE and PP as matrix have been used in producing the test samples. The material properties of fibre and matrix material used to prepare the pipe specimen in this study were as shown in Table 1. All the samples were produced by the factory using the extrusion process, operated at adjustable speeds (mandrel-rotating die speed /rpm).

A few batches of sample specimens were received from the supplier, denoted as samples GPP1, GPP2, GPE1, GPE2, GPE3, GPE4, GPE5, MDPE6, MDPE7 and LDPE3. Detailed descriptions of the studied samples are given in Table 2. Generally, the GPP sample specimens are of 2½-inch (63.5 mm) outer diameter, 3 mm thickness and 6.25 % fibre volume fraction. However, the GPE samples are of 3¼-inch (91.86 mm) outer diameter, 10 mm thickness and fibre volume fraction of 5%, 10% and 20 %.

Three sets of experiments were performed upon these composite plastic pipe sections. In the first, the fibre orientation of the pipe samples was examined. Parallel and perpendicular surface to axis of samples were polished up to 6  $\mu\text{m}$ . Additionally, Optical Microscopy Analyser (MAGISCAN and GENIAS software) was used to determine the distribution of fibre orientation. Secondly, samples were tested according to the ASTM- 3039 and BS 2782: Part 3: Method 320A to identify their mechanical properties. Tensile test was carried out by using the universal testing machine Instron 4507, at cross-head speed of 12.7 mm/min. The axial and hoop strain were measured using two strain gauges mounted on each opposite sides of the specimen. The Young's Modulus (E) was calculated under the stress-strain curves.

Finally, all pipe samples were machined to the required dimension of similar thickness to diameter ratio ( $t/D$ ). The samples were then crushed axially by using the Instron - Universal Testing Machine at

constant speed. The effect of the  $V_f$  and fibres orientation ( $\theta$ ) to the specific energy absorption and mode of failures was analyzed.

**Table 1** Material properties of fibres and matrix materials

Property	E-glass	Polypropylene PP	Polyethylene MDPE	Polyethylene LDPE
Density, $\rho$ (kg/m <sup>3</sup> )	2450	900	955	920
Modulus E (Gpa)	76	1.2	0.43	0.18
Tensile stress, $\sigma$ (Mpa)	400 ksi	35	26	13
Elongation %		> 200	100-300	400-800

**Table 2** Detailed description of samples (GPP, GPE, MDPE and LDPE)

Specimen	Description.	T, mm	OD, mm	ID, mm	t/D, ratio
GPP1	6.26 % Glass and PP and 20 rpm	3	63	57	0.04
GPP2	6.26 % Glass and PP and 20 rpm				
GPE 1A	100 % RTP (20% Glass), 30 rpm	3	63	57	0.04
GPE 2A	1 part RTP, 1 part PE100 (10% Glass) 30 rpm				
GPE 3A	1 part RTP, 1 part PE100 (10% Glass) 15 rpm	4	96	88	0.04
GPE 4A	1 part RTP, 3 part PE100, (5% Glass) 30 rpm	4	96	88	0.04
GPE 5A	1 part RTP, 3 part PE100, (5% Glass) 15 rpm	4	96	88	0.04
MDPE6A	No Glass PE100	4	96	88	0.04
MDPE7A	No Glass PE100	4	96	88	0.04
	Control end, 60 rpm				
LDPE3	Low Density Polyethylene	2	72		0.04

### 3.0 RESULTS AND DISCUSSION

#### 3.1 Fibre Orientation and Volume Fraction

There are several methods to determine the individual orientation of fibres in composite materials. These are optical micrographic, X-ray observation, scanning electron microscopy and wide-angle X-ray diffraction, etc. [18, 22, 23, 24, 25]. In this study, the microphotography technique, which uses an optical microscope and camera, was used in this study.

Figures 1a and 2a show the distributed fibre orientation in the parallel plane of selected samples. The majority of the fibres appeared as small circles, which meant that the fibres were predominantly aligned along or near to the direction of the axis. However, the visual observation of the GPP and GPE composite pipes (Figures 1b to 2b) showed that the majority of planar cross-sections of fibres were in ellipse shapes.

The angles of the fibre orientation at various depths (R/Ri) through pipe thickness were measured, and the average at each point was determined by measuring a number of fibres. The orientation of the ellipse  $\alpha$  produced by the intersection of the fibre was measured directly from the picture. However,  $\beta$  and  $\theta$  angles were obtained from the geometry of the ellipse (Figure 3). This method of experiment is adopted by Bilgin and Sobky [23] and Hull [24].

The distribution of fibre orientation for each of the samples was measured and recorded in Table 3. Generally, it was observed that most of the fibres were distributed randomly. However, 45% to 60% of them were seen to be aligned in a similar direction. The average angles of most of fibres at different thicknesses of the pipes are shown in Figure 4a. It can be seen that the  $\alpha$  angle is slightly bigger near to the inner surface (9° to 22°), slowly decreases in the middle (7° to 18°) and gradually increased to the largest angle near to the outer surfaces (15° to 25°) of the pipes. In addition, the trend of the fibre

orientation with respect to the axial direction of the pipe is presented in Figure 4b. As can be seen, the  $\theta$  angle is between  $55^\circ$  to  $75^\circ$  at the inner surface, and gradually declines to  $45^\circ$  to  $70^\circ$  at the outer surface of the pipes.

The trend of the distribution angle,  $\theta$ , within the R/Ri ratio of the composite pipe samples is found to be related to the speed (rpm) and the fibre volume fraction ( $V_f$ ) during the extrusion process. It can be seen clearly in Figure 4. The GPE4 (5%  $V_f$  / 30 rpm) and GPE2 (20%  $V_f$  / 30 rpm) specimens displayed bigger value of the distribution  $\theta$  compared to the GPE5 (5%  $V_f$  / 15 rpm) and GPE3 (20%  $V_f$  / 15 rpm) specimens, respectively. A similar trend is observed for the GPE1 (20%  $V_f$  / 30 rpm) and (10%  $V_f$  / 30 rpm), while the GPE1 (bigger  $V_f$ ) displayed bigger  $\theta$  angle in the inner and outer surface of the pipes. However, the  $\theta$  angle in the middle surface was seen as not stable, while it may possibly affect the fibres' volume fraction or the rotational speed of the process.

The results indicated that the extrusion process parameters such as rotation speed of mandrel and fibre volume fraction will cause some effects on the orientation of fibres through the thickness of the composite plastic pipes. These results are consistent with previous research (Bilgin and El-Sobky [23], Jian Lui and El-Sobky [25]).

### 3.2 Mechanical Characterization and Tensile Behaviour

The mechanical properties such as axial and hoop modulus calculated from the stress-strain curves are shown in Table 3. Observation shows that they failed a brittle fracture, which occurred at the sudden drop on the stress-strain curves. It was observed that the maximum stress  $\sigma_a$ , and Young's Modulus  $E_a$ , in the axial direction of the sample GPP1/ $\theta$ -70° (37.5 Mpa, and 1299 Mpa) are slightly

lower compared to the sample GPP2/ $\theta$ -60° (41.2 Mpa and 1573 Mpa), respectively. However, the mechanical properties, such as tensile strength and modulus of the GPP composite pipes, were much higher (between 17% – 35 %) compared to the polypropylene (PP) matrix material.

The distribution of fibre orientation for each of the samples was measured and recorded in Table 3. Generally, it was observed that most of the fibres were distributed randomly. However, 45% to 60 % of them were seen to be aligned in a similar direction. The average angles of most of fibres at different thicknesses of the pipes are shown in Figure 4. It can be seen that the  $\alpha$  angle is slightly bigger near to the inner surface ( $9^\circ$  to  $22^\circ$ ), slowly decreases in the middle ( $7^\circ$  to  $18^\circ$ ) and gradually increased to the biggest angle near to the outer surfaces ( $15^\circ$  to  $25^\circ$ ) of the pipes. In addition, the trend of the fibre orientation with respect to the axial axis of the pipe is presented in Figure 4b. As can be seen, the  $\theta$  angle is between  $55^\circ$  and  $75^\circ$  at the inner surface, and gradually declines from  $45^\circ$  to  $70^\circ$  at the outer surface of the pipes.

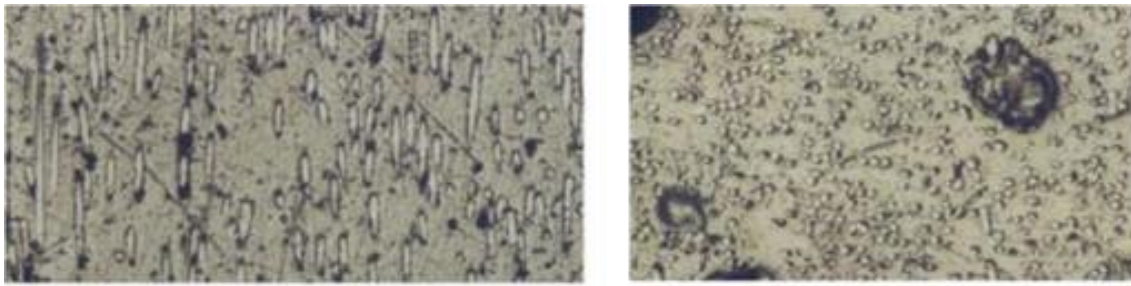
Typical axial and hoop modulus curves for the GPE with different  $\theta$  and  $V_f$  are shown in Figures 5a and 5b, respectively. Both axial and hoop modulus ( $E_a$  and  $E_\theta$ ) slightly increased with increasing  $\theta$  from  $55^\circ$  to  $75^\circ$  (1.4 Gpa and 2.5 Gpa to 1.6 Gpa and 3.2 Gpa), and decreased gradually in between  $75^\circ$  and  $80^\circ$  (1.2 Gpa and 3.1 Gpa), respectively. However, some significant increase of the  $E_\theta$  was defined from the  $\theta$  of  $70^\circ$  to  $75^\circ$  (peak 3.2 Gpa), and reduced gradually to  $\theta$  of  $80^\circ$  (3.1 Gpa). It was identified that the value in hoop direction was almost double the axial modulus. It might possibly be an effect of the distribution of fibres and the  $\theta$  angle (i.e. most of the  $\theta$  angle were close to hoop direction).

**Table 3** Measured angle and mechanical properties of GPP and GPE composite plastic pipe (experimental results)

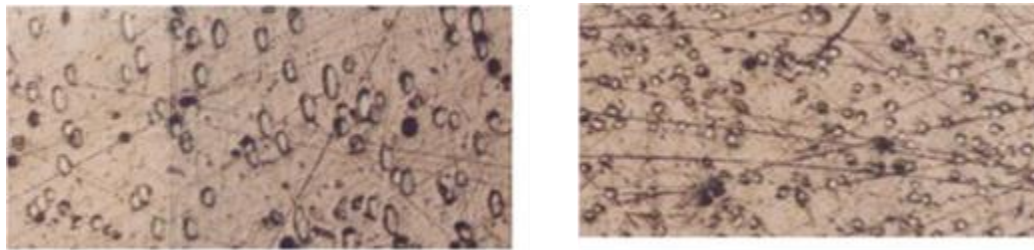
Samples	$V_f\%$	$\alpha$	$\beta$	$\theta$	Axial Modulus ( $E_a$ / Mpa)	Hoop Modulus ( $E_\theta$ / Mpa)
GPP1	6.25	20	20	70	1297	2001
GPP2	6.25	23	30	60	1573	1960
GPE1A	20	20.5	14.2	75.8	1590	3164
GPE1C	20	17.2	16.5	73.5	1520	2886
GPE2B	10	14.7	18.1	71.9	1335	2501
GPE2C	10	23.6	31.4	58.6	1441	2045
GPE3B	10	12.8	12.8	77.2	1215	1951
GPE4B	5	11.9	11.5	78.5	1214	3137
GPE4C	5	17.0	17.0	73	73	3285
GPE5C	5	13.8	13.8	76.2		4509

The graph also indicates the trend of the axial modulus was increased constantly with increasing of  $V_f$  5 % to 20 %. However, the hoop modulus is

highest at the 5%  $V_f$  (4.5 Gpa), decreases significantly at 10% (2.0 Gpa), and gradually increases at 20% (3.0 Gpa).



a) b)  
**Figure 1** Fibre cross-section area of sample GPE1B a) perpendicular and b) parallel to axis



a) b)  
**Figure 2** Fibre cross-section area of sample GPE2B a) perpendicular and b) Parallel to axis

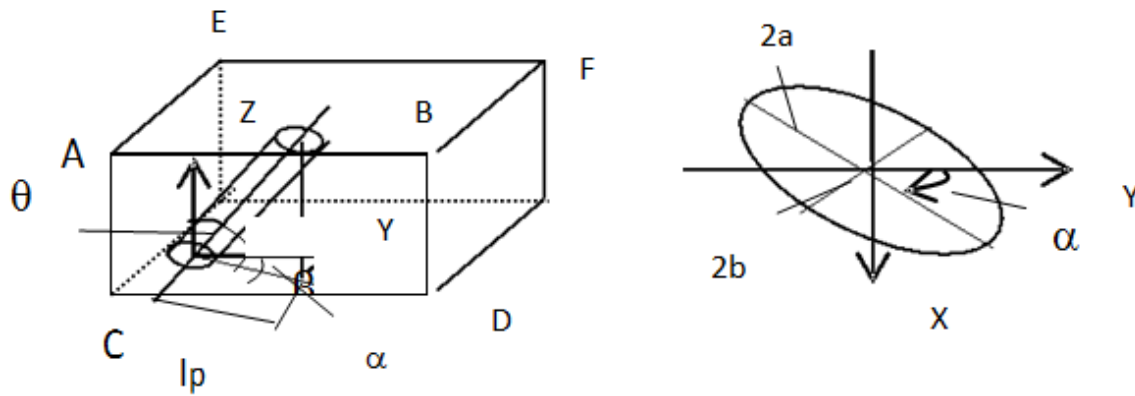


**Figure 3** Experimental method to determine fibre orientation [24]

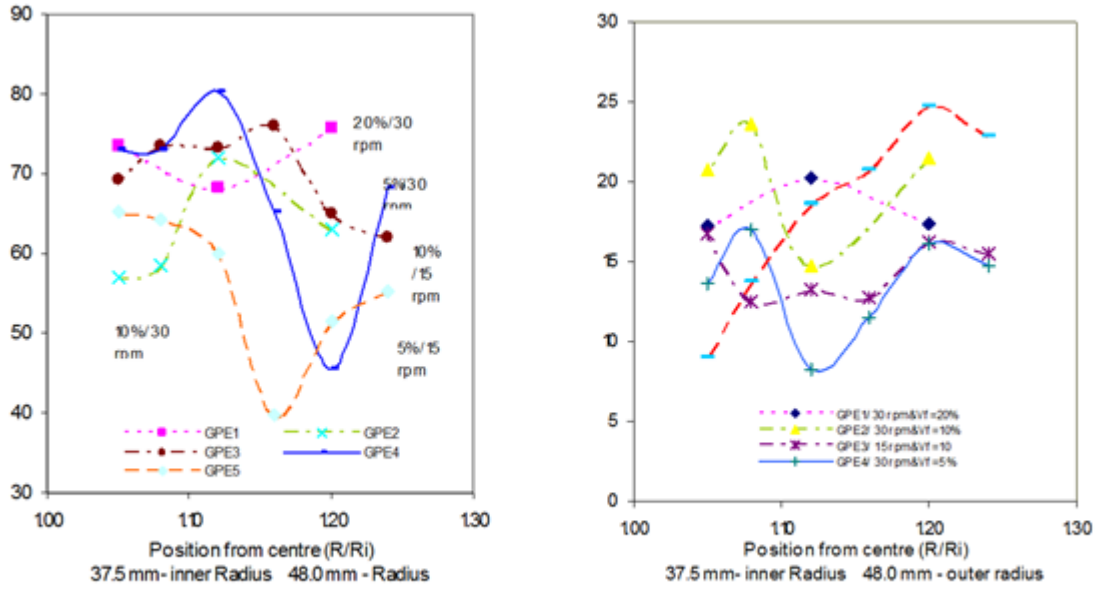


Figure 4 Distribution of the a) average  $\theta$  angle and b) average of  $\alpha$  refer to the R/Ri of GPE samples

3.3 Quasi-Static Test

Selected samples were lathe machined to 115 mm length and t/D ratio of 0.04. One end was machined to 45° chamfer to initiate the progressive crushing [24]. The pipe samples were crushed in axial compression between the flat platen of the Instron Testing Machine, model 4507 at a constant speed of 20 mm/min. Two samples each of the pipes were

tested, with crushing distances approximately 75 to 90 mm. Specific energies ( $E_s$ ) were calculated from the graphs under the load/displacement curves, as described in [24]. The criterion was adopted because the initial slope of the load/displacement curves was different for various samples. A few sets of photographs were taken during the compression of the pipes to assist in understanding and observing the factor of failure.

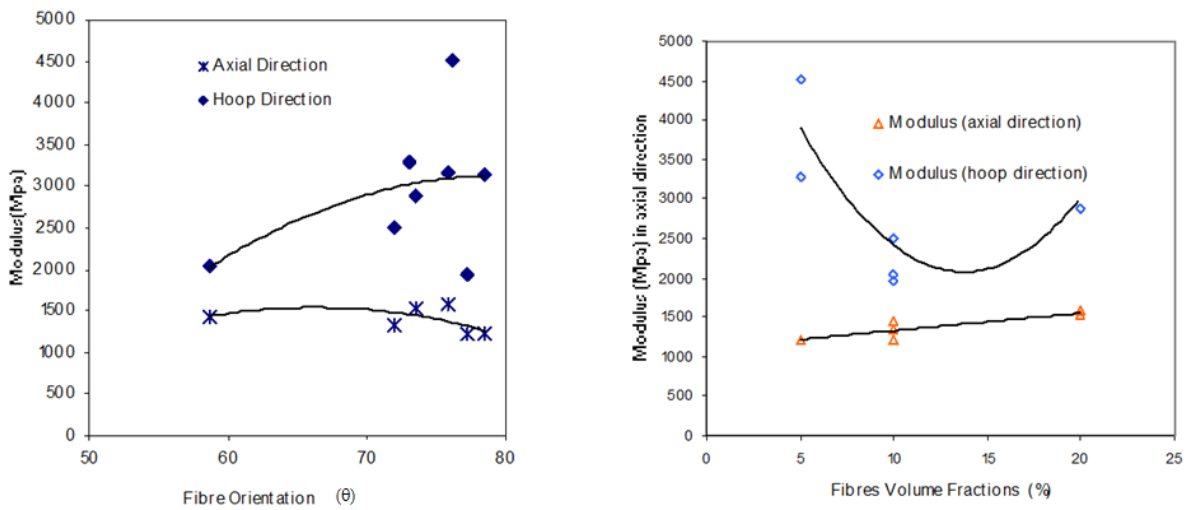


Figure 5 Typical axial and hoop modulus a) different  $\theta$  angle and b) different  $V_f$  of GPE sample

### 3.4 Observation of Collapse Mode

Figure 6 shows the typical load-displacement curves and collapse deformation of the GPP pipes under the quasi-static test, respectively. It was observed that the sample starts collapsing from the chamfer end by bending the chamfer edge inwards, forming and expanding the ring near the chamfer edge. The curves are irregularly serrated, with the maximum amplitude of serrations were within 20 to 24 kN, and the difference between maximum and minimum is almost 10 kN. It was observed that all the specimens appeared to show similar collapse mode characteristics during the crumpling process.

The collapse progresses downwards and causes the cross-section area to increase forming a 3-lobe mode of buckle. The following layers were performed immediately after the first and sit on the other following layer. The buckling mode was taking place at  $60^\circ$  differences from one to the other. The local fracture was also identified as occurring during the crushing, while it may even be possible to be affected by the fibres. Most of the GPP samples collapsed in 3 rings of the 3-lobes or mixes (2 or 3 lobes) of the non-axis-symmetric mode. The 3-D visual observation of collapse mode phenomena of GPP pipes under quasi-static test is shown in Figure 6b. It can be seen that the local fracture and tearing accrued during the progressive folding process.

Some different collapsed modes on the GPE composite pipe that occurred were related to the different  $V_f$  and  $\theta$ . The sample GPE 1, which has 20 %  $V_f$  and about  $75^\circ$  of  $\theta$ , failed in buckling and fragmentation modes (as a brittle material). It was observed that the sample starts collapsing from the chamfer end by bending the chamfer edge inwards,

forming and expanding the ring near the chamfer edge. The collapse progresses downwards and causes the cross-section area to increase, forming a 3-lobes mode of buckle, and followed by fragmentation. The fragmentation started to take place in a short time after folding and formed debris. The debris was folded either inwards or outwards of the pipe and broke into or out of the pipes. This happened continuously until the end of the crushing (Figures 7a and 7b).

The GPE 2 and the GPE 3 samples, with content of 10%  $V_f$ , collapsed in non-axis-symmetric and formed the 2 rings of the 3-lobes, with the local fracture in the inner and outer surfaces of the samples. It was observed that the local fracture started in the inner surface along the folding line and followed to the outer surface of the sample (Figures 7c and 7d).

The GPE 4 and GPE 5 samples, with content of 5 %  $V_f$  collapsed in the non- axis-symmetric mode, with either 2 rings of the 3-lobes mode or a ring of the 3-lobes and a ring of the 2- lobes. However, the only minor local fracture occurred along the folding line in the inner surface (Figures 8a and 8b).

The MDPE or PE 100 (MDPE6B, MDPE7B) samples (plastic pipes without fibres) collapsed in the non-axis-symmetric mode with 2 rings of the 3-lobes only. A minor difference was found between these samples. The MDPE6B collapsed with the 3 lobes without any local fracture, whereas the MDPE7B collapsed with the 3 lobes and the minor local fracture on the folding line of the outer surface (Figure 8c).

Many voids were clearly visible, surrounding the surface of the MDPE7B sample, which might be a possible effect of the local fracture that occurred.

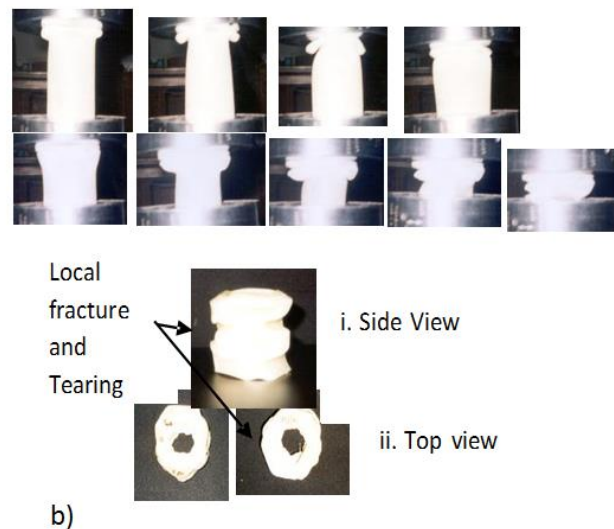
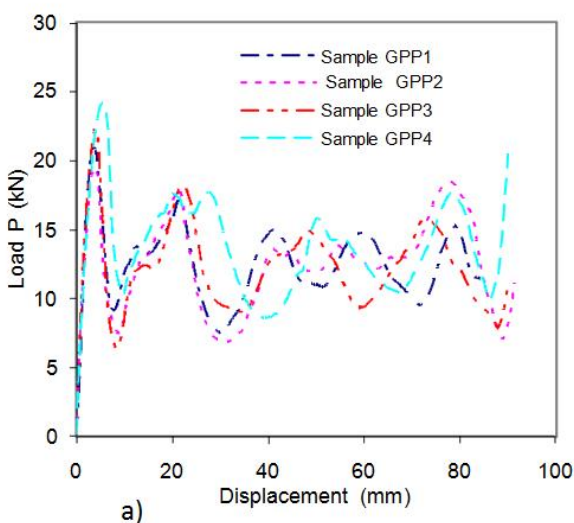


**Figure 6** a) Typical load-displacement curves and b) Collapse progress of GPP composite pipe

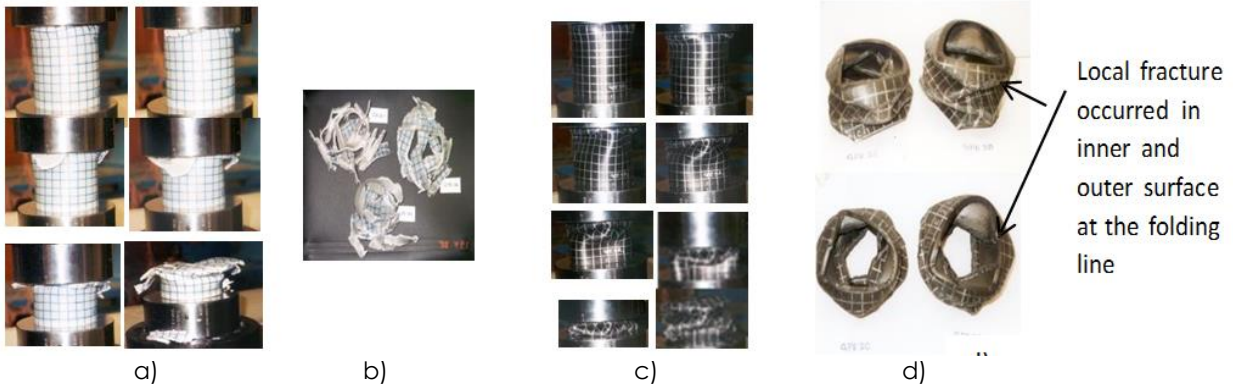


**Figure 7** a) Collapse progress and b) Collapse mode of the GPE composite pipe sample ( $V_f$  20 %) c) Collapse progress and d) Collapse mode of the GPE composite pipe sample (GPE2 and GPE3B-  $V_f$  10 %)



**Figure 8** a) Collapse progress, b) Collapse mode of the GPE 4 and GPE 5 ( $V_f$  5%) and c) Collapse mode of the HDPE 6 and MDPE 7 (non fibre)

## 4.0 CONCLUSION

In this paper, experimental investigation of the effect of fibre orientation and volume of fraction to the axial and hoop modulus of GPP and GPP composites and their collapse modes subjected to axial static loading have been presented and discussed in detail. The following concluding remarks may be drawn;

- The optical microscopic experimental study has shown that most of the fibres were distributed at a similar angle depending on  $R/R_i$  ratio. The  $\theta$  angle displayed bigger volume in the inner surface and smallest in outer surface of pipes.

- The results from the experiment revealed that typical axial and hoop modulus ( $E_a$  and  $E_\theta$ ) of GPP and GPE pipes slightly increased with increasing of  $\theta$  from  $55^\circ$  to  $75^\circ$  and decreased gradually in between  $75^\circ$  and  $80^\circ$ . The axial modulus was increased constantly with increasing of  $V_f$  5 % to 20 %. However, the hoop modulus is highest at the 5%  $V_f$  (4.5 Gpa), which decreases significantly at the 10% (2.0 Gpa), and gradually increases at the 20% (3.0 Gpa).

- The observation from the experimental result has indicated that the collapse mode characteristic

of the composite plastic pipes is generally related to the mechanical properties and strength of the materials. Moreover, fibre volume fraction and fibre orientation seem to be the main factors that might affect the failure mode of composite pipes during axial crushing. The pipe samples that contain more  $V_f$  and  $\theta$  angles collapsed as brittle failure modes (buckling and fragmentation), while those with less  $V_f$  and  $\theta$  angles collapsed in non-axis-symmetric (diamond) with local fracture. Moreover the local fracture disappeared when the  $V_f$  content decreased.

## References

- [1] Hull, D. 1983. Axial Crushing of Fiber Reinforced Composite Tube. In Structural Crashworthiness, N. Jones and T. Wierzbicki, Butterworth, London. 35-118.
- [2] Haug, E. and Rouvray, A. D., Crush. Response of Composite Structures. *Engineering System International*. SA, 94578 Rungis-Cedex, France.
- [3] Thornton, P. H. 1979. Energy Absorption in Composite Structures. *J. Composite Mat.* 13: 247-262.
- [4] Farley, G. L. 1986. The Effect of Fibres and Maximum Strain on the Energy Absorption of Composite Materials. *J. Composites Mat.* 20: 322-334.



- [5] Schmueser, D. W. and Wickcliffe, L. E. 1987. Impact Energy Absorption of Continuous Fibre Composite Tubes. *J. Eng. Mat. Tech.* 109: 72-77.
- [6] Price, J. N. & Hull, D. 1988. Crushing Behaviour of Square Section of Glass Fibre Polyester Tube. In *How to Apply Advance Composite Tech. ASM International.* 53-61.
- [7] Price, J. N. & Hull, D. 1987. Axial Crushing of Glass Fibre-Polyester Composite Cones. *Composite Sc. Tech.* 28: 30-211.
- [8] Thornton, P. H. and Jeryan, R. A. 1988. Crash Energy Management in Composite Automotive Structures. *Int. J. Impact Eng. Mat.* 7: 167-180.
- [9] Mamalies, A. G., Manolakos, D. E. and Viegelahn, G. L. 1989. The Axial Crushing of Thin PVC Tubes and Frusta of Square Cross Section. *Int. J. Impact. Eng.* 8: 64-241.
- [10] Carruthers, J. J., Kettle, A. P. and Robinson, A. M. 1998. Energy Absorption Capability and Crashworthiness of Composites. *Appl. Mech. Rev.* 51: 10.
- [11] Mamalies, A. G. Review Crashworthy Capacity of Composite Materials. *Composite Structure.* 37: 109-134.
- [12] Hull, D. 1991. A Unified Approach to Progressive Crushing of Fibre-reinforced Composite Tubes. *Composite Science and Technology.* 40: 377-421.
- [13] Farley, G. L. 1983. Energy Absorption of Composite Materials. *J. Comp. Mat.* 17, 267-279.
- [14] Thorton, P. H. and Edwards, P. J. 1982. Energy Absorption in Composite Tubes. *J. Comp. Mat.* 16: 521-45.
- [15] Farley, G. L. and Jones. 1992. Crushing Characteristic of Continuous Fibre-Reinforced Composite Tubes. *J. Comp. Mat.* 26: 37-50.
- [16] Farley, G. L. 1986. The Effect of Fibre and Matrix Maximum Strain on Energy Absorption of Composite Materials. *J. Comp. Mat.* 20: 322-334.
- [17] Mamalies, A. G. 1991. On the Axial Crushing of Fibre-Reinforced Composite Thin-Walled Conical Shell. *Int. J. Vehicle Des.* 12: 450-467
- [18] Private communication with El-Sobky, H.
- [19] Farley, G. L. 1986. Effect of Specimens Geometry on Energy Absorption Capability of Composite Materials. *J. Comp. Mat.* 20: 390-400.
- [20] Farley GL and Jones RM (1992) Crush characteristic of composite tubes with near elliptical cross-section. *J. Comp. Mat.* 13, 37-50
- [21] Isaac, M. D. and Ori Ishai. 1994. *Engineering Mechanics of Composite Materials.* New York, Oxford.
- [22] Doshi, S. R., Dealy, J. M. and Charrier, J. M. 1986. Flow Induced Fibre Orientation in an Expanding Channel Tubing Die. *Polymer Engineering and Science.* 26: 486-478.
- [23] Bilgin and Sobky. 1981. Extrusion of Pipes Using Rotating Die System. Msc. Thesis, Umist, Manchester, England.
- [24] Hull, D. 1981, 1996. *An Introduction to Composites Materials.* 2nd. Edition. Cambridge.
- [25] Jian Liu and Sobky. 1996. A Study of Fibres Orientation in Composite Melt Processing. Mphil Thesis, UMIST, Manchester England.